

# Chapter 4

## 4 Carbon Quantum Dot as Electron Transporting Layer in Organic Light Emitting Diode

### 4.1 Introduction

#### 4.1.1 Fundamentals of OLED

Organic Light Emitting Diodes (OLEDs) are light emitting devices that are being used as displays in smartphone, TV's, lighting etc[145][118][146]. OLEDs are very flexible, have large color range and contrast, fuller viewing angles and consume low power[147]. All these features helped them to capture a huge market share for display technologies in recent years[148]. In an OLED, electrons and holes are injected into the active electroluminescent material packed in between two electrodes, where they recombine to emit light. To improve the charge recombination in the EML layer, usually a hole transport layer (HTL) and an electron transport layer (ETL) is inserted between the emissive layer/anode and emissive layer/cathode respectively. These layers improve charge carrier extraction and block opposite charge carriers thereby suppressing charge recombination at the emissive layer–electrode interface. In OLEDs, the injection of electrons is more important than that of holes because the electron mobility in organic semiconductors is lower than the hole mobility[149][150][151]. The optoelectronic properties of the HTL and ETL thereby influence the efficiency of the device.

### **4.1.2 Hole and electron transport materials in OLED**

Tremendous research has been conducted to determine the best material for ETL and HTL in photovoltaic devices. HTL materials need to have a high work function to have efficient hole injection from anode. Typical materials used as HTL include organic semiconductors/polymers (PEDOT:PSS, TAPC, TCTA, CPB, CuPc) and transition metal oxides ( $V_2O_5$ ,  $MoO_3$ ,  $NiO$ ) [152][153][154][155]. PEDOT:PSS is one of the most commonly-used HTL layers in organic photovoltaic devices due to its high conductivity and high optical transparency. Hybrid composite materials made up of more than one organic molecules or composite of organic molecules with quantum dots have also been used as HTL material [156]. ETL materials need to have a low work function to provide low barrier for electron injection from the cathode. In addition ETL materials should have reasonably high electron mobilities and must be chemically stable. There are many organic molecules/polymers (Alq3, TPBI, BCP) and inorganic oxides (LiF, ZnO,  $TiO_x$ ) that has been used as ETL [157][158]. Some these materials like doped  $MoO_x$  and  $VoO_x$  can be used both as hole and electron transport layers [159]. Optimum choice of HTL and ETL materials is necessary to get high efficiency optoelectronic devices.

### **4.1.3 Properties of QDs**

Quantum dots (QDs) are a versatile group of materials whose properties can be easily tuned by varying the shape, size, composition and surface functional groups. Size and shape engineering of QDs can be used to tune the band gap, charge mobilities, optical luminescence [160]. Bowers et. al. demonstrated that magic sized CdSe QDs have very broad white light emission (420 nm to 710 nm) compared to other semiconductor CdSe QDs [161]. Yuan et. al. demonstrated that triangular carbon quantum dots exhibited narrow multicolored

bandwidth emission with high quantum yields compared to other CQDs[162]. QDs in the shape of sphere, cube, rods, discs, tetrapods, octapods etc. with varying properties have been also synthesized[163][164][165][166]. QDs has been used as the active materials in many solar cells. In QDs, surface chemistry plays an important role in determining its electronic properties. The work function of QDs can be tuned easily by surface functionalization, Kroupa et. al demonstrated that the band edge positions of PbS QDs can be tuned by 2eV using surface functionalization[167][168][169]. Since the one of the most important requirement for charge transport layer is work function, QDs can be used both as HTL and ETL.

Recently Carbon Quantum Dots have caught the attention of researchers worldwide due to exceptional electronic and optical properties with tunable band gap, excitation dependent emission, high fluorescence quantum yields, upconversion, low toxicity, chemical inertness and more[170][171][68]. Most CQDs have an amorphous or crystalline core (with predominantly  $sp^2$  hybridized carbon) terminated by surface functional groups[170][171][68][172]. These surface functional groups (mostly oxygen or nitrogen containing species) dominate its surface chemistry making it highly soluble in polar solvents like water and also introducing surface states in the band gap which influences its electronic and optical properties[173]. It has been reported that stronger photoluminescence (PL) of CQDs can be observed by replacing the oxygen-containing surface functional groups with nitrogen-rich groups[174][175]. These functional groups can be introduced during synthesis or post synthesis with additional surface treatment. The chemical nature of these functional groups strongly dependent on the specific synthesis methods and precursors used[176][177][178]. CQDs are used in numerous applications in solar cells, LEDs, optical sensors, photocatalysis, bioimaging etc [179]. CQDs have been used in emissive layers in LED

and as hole transport layer in organic solar cells[180]. In this article, we report the use of CQDs, synthesized with one step hydrothermal process using banana leaf precursor, as Electron transporting layer (ETL) in OLED.

## 4.2 Results and Discussion

### 4.2.1 Optical, structural and morphological characterization of CQDs

In Figure 4.1 (a) UV-Vis spectra of CQDs dispersed in water shows maximum absorption in the UV region at 250 nm and negligible absorption in the visible region. Weak absorption peaks are also observed at 320 nm and 400 nm. The peak at 250 nm and 320 nm is usually attributed to  $\pi$ - $\pi^*$  transition of C=C bond and n- $\pi^*$  electronic transition of C=O & C=N bonds respectively. The long absorption tail extending into the visible region is due to the mid gap surface state produced by functional groups anchored at the surface. FTIR was used to determine the surface functional groups adsorbed on CQDs. FTIR spectra in Figure 4.1 (b) indeed shows the presence of O-H, C=C and C=O double bonds. A broad band centered at  $3415\text{ cm}^{-1}$  was observed which is characteristic of O-H or N-H stretching vibration modes. A small peak at  $2935\text{ cm}^{-1}$  is caused by the stretching vibration of aliphatic C-H group. A small peak at  $2360\text{ cm}^{-1}$  may be caused by  $\text{sp}^3$  bonded C-C or C-N groups. The sharp peak at  $1635\text{ cm}^{-1}$  is assigned to the bending vibration modes of  $\text{sp}^2$  hybridized C=C bonds. The small sharp peaks at  $1384\text{ cm}^{-1}$  and  $1311\text{ cm}^{-1}$  are caused by aliphatic C-H and O-H bending of the phenolic and carboxylic groups. The peak at  $1060\text{ cm}^{-1}$  is assigned to either ether stretch (C-O) or C-H in-plane deformation. Finally, at low wavenumbers at  $786$  and  $668\text{ cm}^{-1}$  are ascribed to out-of-plane bending of aromatic C-H bonds. These results indicate that the core of CQDs is made of both  $\text{sp}^2$  and  $\text{sp}^3$  bonded carbon atoms with surface rich in oxygen and nitrogen-containing functional groups which makes them highly soluble and stable in water.

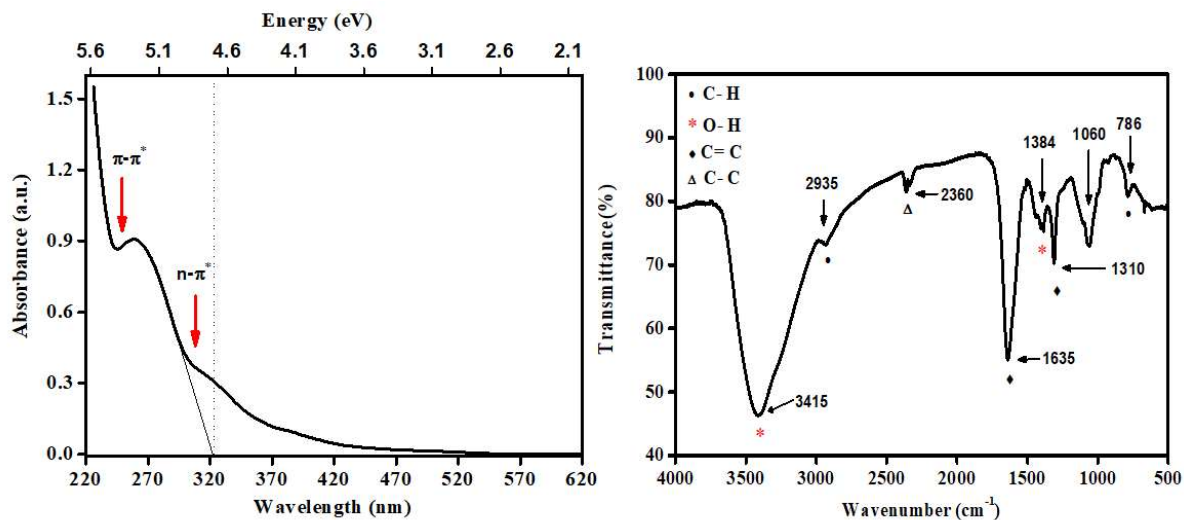


Figure 4.1 (a) UV-Vis absorption spectra of CQD in aqueous solution and (b) FT-IR spectrum of CQDs, showing characteristic IR active modes for O-H, C-H, C=C, C-C and C = O groups

The PL data of the CQDs revealed excitation-dependent fluorescence with maximum emission intensity at 425 nm giving strong blue fluorescence when excited at 320 nm excitation wavelength (Figure 4.2 (a)) with full width half maxima of 106 nm. PL spectra of CQDs are usually very broad since the core, defects and diverse surface functional groups act as multiple photoluminescent centers. Song et. al. investigated the effect of size on the PL of graphene quantum dot (GQD). They reported that as size of GQDs increased due to the presence of more functional groups on larger GQDs, the PL emission peak was red shifted and was thus broadened [181]. Yuan et. al. demonstrated that highly crystalline triangular CQDs of size 3 nm exhibit very narrow PL peaks (fwhm 20 nm) [162]. To study the physical and morphological characteristics of the CQDs, TEM measurements were conducted. The synthesized carbon dots were amorphous and round-like in shape. The average size of the CQDs are 4-6 nm (Figure 4.2 (b)). In addition to the presence of functional groups, the amorphous core comprised of both  $\text{sp}^2$  and  $\text{sp}^3$  carbon also broadens the PL peak. Figure 4.2

(c) shows the PL decay curve of the CQDs. After fitting the lifetime of decay comes out to be 1.2 ns.

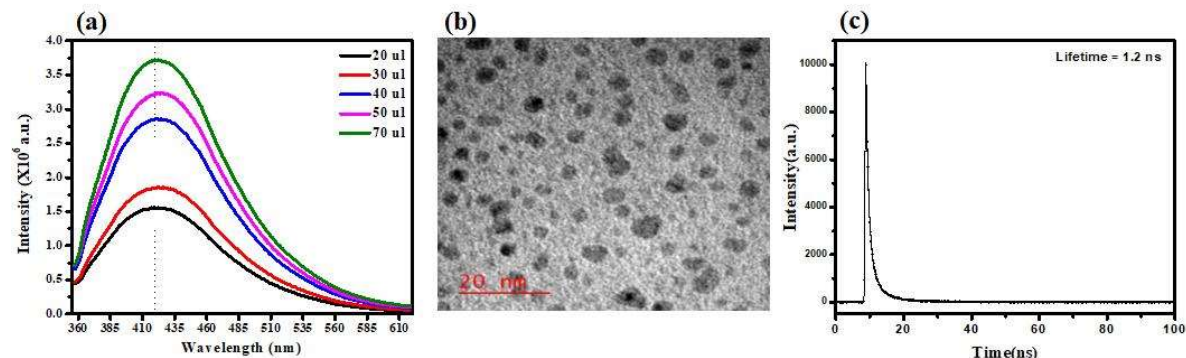


Figure 4.2 (a) PL spectra of CQD aqueous solution at excitation wavelength of 320 nm (b) TEM image of CQDs (c) PL decay curve of CQDs

#### 4.2.2 Device structure of OLED

The schematic of the device structure and energy level alignment for ITO/PEDOT: PSS/PFO/LiF/Al, ITO/PEDOT: PSS/PFO/CQD/LiF/Al have been given in Figure 4.3 (a). From literature we know that the HOMO (LUMO) value for PEDOT: PSS and PFO are 5.2 eV (2.4 eV) and 5.8 eV (2.8 eV) respectively. We can conclude that that electron and holes are easily injected into this device directly to PFO.

#### 4.2.3 Electrical characterization of OLED

Prototype OLED devices with pristine PFO and CQD as ETL have been characterized by current versus voltage characteristics, as shown in (Figure 4.3 (b)). The threshold voltages for Device A, B and C are 3V, 6V and 8V respectively. Device C with CQDs as ETL has lower turn on voltage than Device B. Introduction of CQD as the ETL reduces the barrier for electron

injection which in turn lowered the turn on voltage. The recombination of electrons and holes in the active layer PFO results in electroluminescence (EL) under bias.

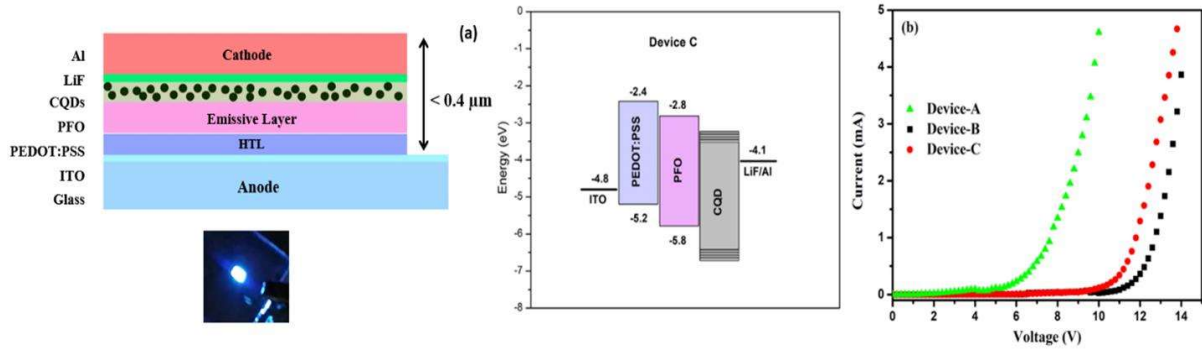


Figure 4.3 (a) Schematic diagram of energy level alignment of OLEDs (b) Current Voltage Characteristics of OLEDs

The electroluminescence (EL) spectra of the Pristine PFO Device and PFO-CQD Device as function of operating voltage are shown in Figure 4.4 . For the device, with PFO the EL spectra show prominent peaks at 435 nm, 460 nm and 489 nm with, highest intensity at 460 nm. All these peaks exhibit a red shift compared to the peak position reported for pristine PFO in literature. There is also a weak peak at 525 nm. For some operating voltages, Device C exhibits more intense EL peaks. In both devices with increasing voltage, the intensity of the peaks increase proportionately. However for Device C at 15V the intensity of peak at 489 nm increases manifold reaching saturation levels. Although Device A has the lowest threshold voltage at 2.5 eV, it does not exhibit any electroluminescence. These results indicate that CQDs can be used as efficient electron transport layers in OLED.

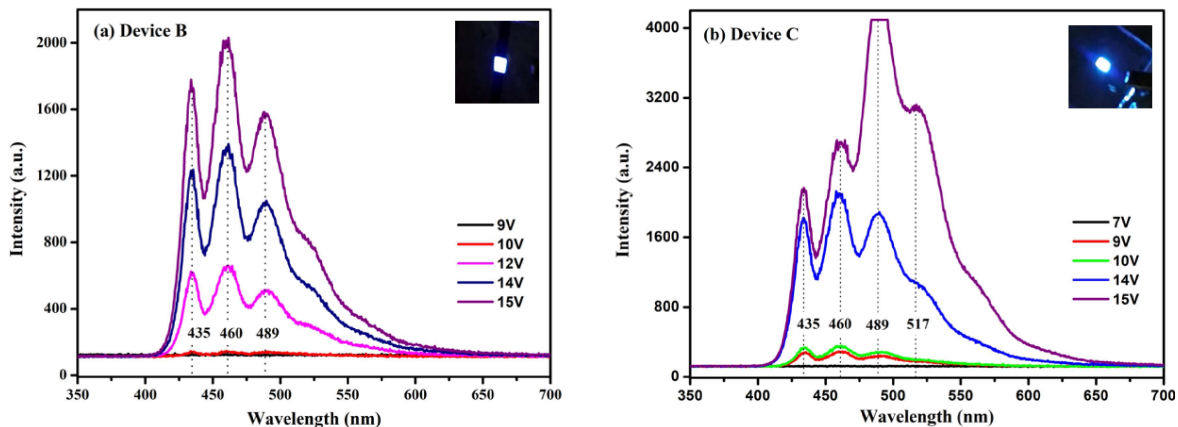


Figure 4.4 Electroluminescence spectra of OLEDs as function of operating voltage (a) Device B: ITO/PEDOT:PSS/PFO/LiF/Al (b) Device C: ITO/PEDOT:PSS/PFO/CQD/LiF/Al (inset shows brightness of OLED at 15V)

### 4.3 Conclusions

In summary we have, for the first time, prepared carbon quantum dots from banana leaves green and facile one-pot hydrothermal method. The average diameter of CQDs is approximately 4- 6 nm, exhibit excitation dependent PL emission in aqueous solution. The incorporation of solution processable CQD into OLEDs as the cathode interfacial layer for electron transporting, excellent electron transport is necessary to improve the electroluminescent efficiency, because the difference between LUMO level in CQDs and the Fermi energy of LiF/ AL is significantly large, which is partially enhanced by the solution process of ETL layer before LiF/AL. We demonstrated that the use of CQD improving the electron donating ability in OLED. The layer of CQD as ETL has a better turn-on voltage, quantum efficiency, conductivity, and maximum luminescence.